Institute of Paper Science and Technology
Atlanta, Georgia

IPST TECHNICAL PAPER SERIES

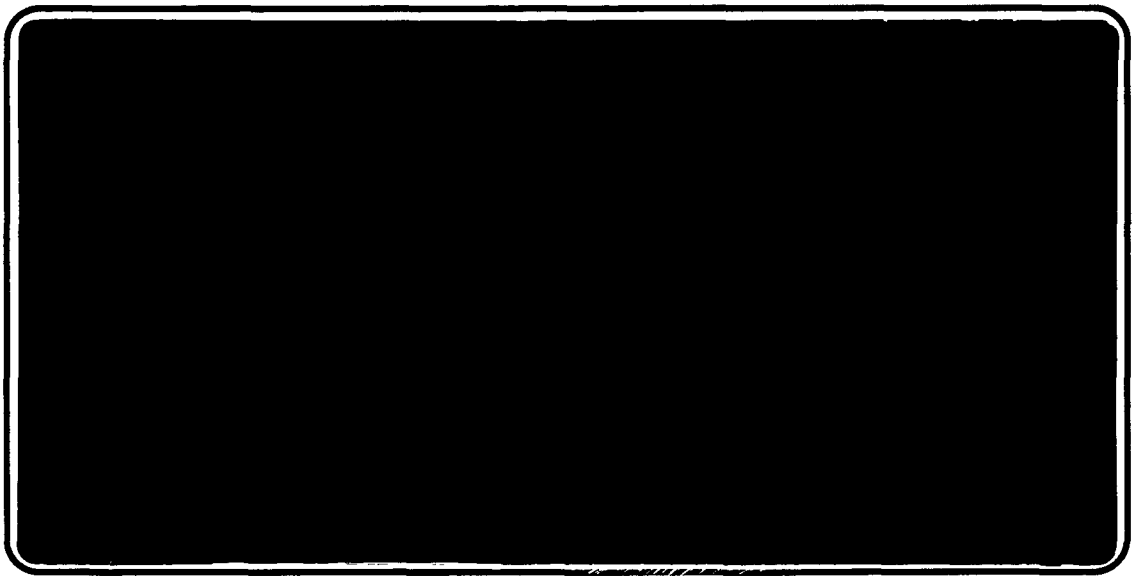

NUMBER 386

CELL WALL SULFUR DISTRIBUTION IN SULFONATED SOUTHERN PINE LATEWOOD—PART 2: EFFECTS OF PROCESS VARIABLES AND MATHEMATICAL MODELING OF INTRAFIBER DIFFUSION WITH REACTION

T.E. HEAZEL AND T.J. MCDONOUGH

JULY, 1991

Cell Wall Sulfur Distribution in Sulfonated Southern Pine Latewood—Part 2: Effects of Process Variables and Mathematical Modeling of Intrafiber Diffusion with Reaction

T.E Heazel and T.J. McDonough

To be presented at
1991 International TAPPI Paper Physics Conference
Kona, Hawaii
September 22–27, 1991

CELL WALL SULFUR DISTRIBUTION IN SULFONATED SOUTHERN PINE LATEWOOD—PART 2: EFFECTS OF PROCESS VARIABLES AND MATHEMATICAL MODELING OF INTRAFIBER DIFFUSION WITH REACTION

T.E. Heazel *
Graduate Student
Institute of Paper Science and Technology
Atlanta, Georgia
USA

T.J. McDonough
Professor
Institute of Paper Science and Technology
Atlanta, Georgia
USA

ABSTRACT

Virtually all commercial chemithermomechanical and chemimechanical pulping systems rely on pretreatment with sodium sulfite to modify the mechanical properties of the double cell wall prior to fiberization. The principal mechanism is believed to involve sulfonation of lignin, which decreases both its modulus of elasticity and the resistance it offers to fiber separation. A direct result is that the amount of damage suffered by the fibers during separation is substantially decreased. A second, equally important result is increased pulp fiber flexibility and conformability.

At any given microscopic locality within the double cell wall, the extent of these effects may be assumed to increase with increasing degree of sulfonation. Consequently, the distribution of sulfonate groups throughout the various cell wall layers can be expected to profoundly affect pulp properties. For example, wood chips in which the middle lamella lignin is softened by extensive sulfonation will tend to fail in the middle lamella, resulting in fibers with a lignin-rich surface. At lower degrees of middle lamella sulfonation, fracture will tend to occur in the outer secondary wall, creating a relatively carbohydrate-rich surface with different bonding characteristics[1]. Increased sulfonation within the secondary wall leads to higher sheet density and strength by improving conformability[2]. It is apparent that if the distribution of sulfonate groups within cell walls could be manipulated, pulp properties could be tailored to end-use requirements.

A necessary step along the path to acquiring this ability is to obtain an understanding of how the distribution depends on process variables. This, in turn, requires a suitable microanalytical technique for the determination of bound sulfur in an extremely narrowly defined region of the cell wall. X-ray microanalysis meets this requirement. Its application to the determination of sulfur at various points within wood cell walls was pioneered by Kolar and co-workers[3]. They used scanning electron microscopy (SEM) with energy-dispersive X-ray analysis (EDXA) to show

* Now with S.D. Warren Co., Westbrook, Maine.

that a particular set of sulfonation conditions gave much higher sulfur concentrations in the middle lamella than in the secondary wall. They were able to say little more than this, however, because of the limited spatial resolution of SEM. To overcome this difficulty, Beatson and co-workers[4] used transmission electron microscopy with EDXA to map sulfur distribution in cell walls of sulfonated black spruce. The higher resolution of this method allowed these workers to isolate cell corner data and to observe the sulfur distribution across the secondary wall. They found a constant ratio of cell corner to secondary wall counts and a flat distribution across the secondary wall for chips which had been cooked after long impregnation at high liquor-to-wood ratio.

Subsequently, we employed scanning transmission electron microscopy (STEM) to relate the cell wall sulfur distribution in Southern pine latewood to sulfonation conditions[5]. Our objective was to find conditions that would result in different cell wall sulfur distributions by studying the effects of Na_2SO_3 concentration and cooking time in low liquor-to-wood ratio (vapor phase) cooks. All of the conditions studied yielded a distribution characterized by a pronounced gradient of bound sulfur across the secondary wall. Sulfur counts decreased from a high value near the lumen to a minimum in the outer secondary wall and then increased toward a maximum in the middle lamella. At that time, we were unable to detect any dependence of the shape of the distribution on the variables studied, and could only speculate with regard to possible reasons for the secondary wall gradient.

The present paper reports the results of continued studies of this phenomenon. The objectives of the more recent work were to continue to search for a means of controlling the bound sulfur distribution and, in addition, to gain a better understanding of the source of the gradient observed earlier. The former objective was pursued by conducting two series of experiments. In the first, we varied the intensity of sulfonation in vapor phase cooks. In the second set of experiments, conducted at a higher liquor-to-wood ratio, we determined the effects of varying pH and time, both separately and together. Both sets of experiments employed an improved chip impregnation technique, and both were rigorously designed and analyzed according to established statistical principles. This was made necessary by the high degree of natural variation between locations within a wood chip, and between chips.

Our earlier analysis of the literature[5] indicated that limitations on intrafiber diffusion may be responsible for the secondary wall gradient. To further examine this somewhat counterintuitive conclusion, we have conducted a more detailed analysis, and we have constructed a mathematical model of diffusion across the cell wall to simulate the process and determine the minimum assumptions necessary to explain the observed distributions on the basis of diffusion limitations.

MASS LOSS

While the present study was in progress, Mary and co-workers at the Pulp and Paper Research Institute of Canada published results demonstrating that, under the conditions of x-ray microanalysis, a significant portion of the sample may be lost as a result of volatilization by the electron beam[6]. Since this mass loss was shown to occur within the first few seconds after exposure to the beam, it has obvious potential implications with regard to the accuracy of the analysis. Consequently, it was necessary to examine the phenomenon and assess its effects under the conditions used in our analyses. The methods used are outlined in the experimental part of the present paper and are described in detail elsewhere[7].

The results generally agreed with those reported by Mary, with the exception that our mass loss levels were somewhat lower. Approximately 40% secondary wall mass loss occurred within the first few seconds of exposure to the beam. Increasing the beam intensity increased the rate, but not the extent of mass loss. Loss of sulfur from the secondary wall was only about one-third as great as the total mass loss, averaging 14% in the samples examined. Total mass loss from the cell corner region was only about one-half as great as that observed in the secondary wall. Because of its relatively small size in the fiber cross sections, the cell corner region did not provide sufficient sulfur counts to properly measure sulfur loss in that region. It was also not possible to determine the distribution of sulfur loss across the secondary wall because of the insufficient sulfur counts that could be acquired from a single pixel during the short time over which mass loss occurred.

In summary, it appears unlikely that sulfur volatilization seriously affected the observed cell wall sulfur distributions. The general level of sulfur loss was relatively low, and there is no reason to believe that it occurred preferentially in any given region of the secondary wall.

EXPERIMENTAL DESIGN AND STATISTICAL ANALYSIS

An important aspect of this study was the design of the experiments and the statistical analysis of the resulting data. Both were necessary to allow valid conclusions to be drawn in the face of extensive natural variation in the raw material at a microscopic level.

The raw material for this study was a Southern pine log from which wood chips (25mm long x 5-10 mm wide x 2 mm thick) were cut from the latewood portion of single annual rings. The long axis of each chip was parallel to the longitudinal axis of the log. The axis traversing the thickness of the chip (parallel to the log's radius) was the radial axis, while the axis traversing the width of the chip was the tangential axis. Consequently, each chip had two large tangential faces (formed by longitudinal and tangential axes) and two transverse faces (formed by radial and tangential axes). For each cooking condition (as defined by time, temperature, pH, liquor-to-wood

ratio and Na_2SO_3 concentration), two cooked chips were randomly selected for analysis. Transverse thin sections were taken from the middle of each chip, and two locations were analyzed within selected sections. One of these was chosen to be near a tangential face of the chip (near the outer edge of the section) and one near the center of the section.

Two different cells were analyzed at each location, and each cell was scanned twice, along closely adjacent lines. The locations of the sites analyzed within each chip are schematically represented in Figure 1.

The analysis of the data decomposed the total variation in the data into individual components attributable, respectively, to each of the cooking variables: interactions, variability between chips, differences between locations (radial positions) within each chip, variability between walls (cells) at the same location and variability between adjacent scans of the same wall.

SULFITE TREATMENT OF WOOD CHIPS

Table 1 gives the results of analyses of the treated wood chips from both sets of experiments. With one exception, the yields were all 95% or greater, making it unlikely that delignification contributed in any major way to the observed bound sulfur distributions. The vapor-phase cooks exhibited the expected dependence of sulfur content on Na_2SO_3 concentration in the treatment liquor. As intended, the more intense (short, high temperature) cook gave about the same sulfur content as the less intense one at the same concentration.

The liquid phase cooks gave an increased sulfur content at the longer cooking time, although a substantial fraction of the sulfur was incorporated during the heatup period, as shown by the relatively high values at zero cooking time. The extent of reaction also depended on pH, being greater in alkaline than in acid medium. This is in accord with existing knowledge of the chemistry and kinetics of lignin sulfonation[8,9].

SULFUR DISTRIBUTIONS

All treatments gave cell wall bound sulfur distributions that had the same general features as those described earlier[5]. One of the features observed in the previous work was a pronounced sulfur gradient across the secondary wall, with higher sulfur concentrations toward the lumen and lower concentrations toward the compound middle lamella (CML). Another feature was a high sulfur concentration in the CML, presumably a result of the higher lignin concentration there. It was seen as a peak in the center of a symmetrical distribution when the data were collected by

moving the electron beam along a straight line joining the lumen of one cell to that of an adjacent cell (Figure 2a).

Because of the extreme thinness of the CML, the spatial resolution of our STEM-EDXA technique was insufficient to resolve it from the adjacent regions when the data were acquired in this fashion. The difficulty was circumvented by scanning along a line from the cell lumen, through the cell corner (CC), and ending at the primary wall of an adjacent cell. This gave CC middle lamella data that were completely resolved from adjacent morphological regions because of the greater thickness of the middle lamella in the CC region. Data obtained in this way are typified by Figure 2b.

Much of the information in a distribution such as that shown in Figure 2b can be summarized by two ratios and a level indicator. The first ratio conveys the steepness of the gradient in the cell wall. It is simply the ratio of the maximum (A) near the lumen to the minimum (B) near the CML. The second, a measure of the degree to which the higher lignin concentration in the middle lamella results in high sulfur concentration, is the ratio of the mean number of sulfur counts in the CC to the minimum, B. The level indicator can be A, B, CC, or the mean number of secondary wall counts, S. S is preferred, since it may be expected to be unaffected by the steepness of the secondary wall gradient at a given total sulfur content. To deal with the experimental variation in the data, and to enable the assignment of meaningful numerical values to A and B, the secondary wall data were first smoothed by polynomial regression, as described earlier[5].

To demonstrate the validity of the STEM-EDXA technique, we sought a correlation between mean secondary wall counts and the sulfur content as determined on the cooked chips by Schoniger flask combustion and ion chromatography. This is shown in Figure 3, from which it is evident that an excellent correlation exists.

EFFECTS OF TREATMENT INTENSITY IN VAPOR-PHASE COOKS

The sulfur distribution data obtained by STEM-EDXA analysis of chip samples from the vapor phase cooks may be summarized in the form of means calculated for each cooking condition, as shown in Table 2. Each is the average of 16 observations (2 chips x 2 radial locations/chip x 2 cell walls/location x 2 scans/cell wall).

The data sets from which these key treatment means were calculated contain other important information. This information consists of the statistical significance of the differences between the Table 2 means, the extent and significance of the difference between the two radial locations, and the hierarchy of variances that characterize the chip-to-chip variability, the variability between cell walls at the same location, and the variability between scans of the same cell wall. The most important of these are contained in the analysis of variance tables appended as Tables A1 through A3.

The overall extent of secondary wall sulfonation is indicated by the mean number of secondary wall sulfur counts, S. As shown in Table 2, it was slightly higher in the short, high temperature cooks than in the less intense cooks conducted for a longer time at a lower temperature. Analysis of variance (Table A1) confirmed the statistical significance of this effect at a confidence level of about 96%. The effect was not detected by wet chemical analysis of entire chips, in spite of the good correlation shown in Figure 3. The discrepancy lies within the scatter of the data points around the line, suggesting that STEM-EDXA provides the better indicator of the overall level of sulfonation in the cell wall. Both methods, however, showed that more sulfur was introduced by increasing the Na_2SO_3 concentration. The analysis of variance confirmed this, and showed that the concentration effect was no different in the short, high-temperature cooks than in the long, low-temperature cooks. It also revealed a high degree of variability between cells; apparently individual fibers differ in their susceptibility to sulfonation for reasons that are not known. This observation is significant and implies the existence of natural limitations on the uniformity of sulfonation that can be achieved in industrial chemimechanical pulping processes.

Of greater interest in the present context was the distribution of bound sulfur within the cell wall, as indicated by the ratios A/B and CC/B. Within this data set, the former was remarkably consistent, at 1.6 ± 0.06, and very similar to the value of 1.59 ± 0.15 we observed in earlier experiments[5]. Furthermore, this ratio, unlike S and CC/B, was virtually the same for all cells examined, regardless of which chip they were located in and where in the chip they were located. The CC/B ratio was more variable, at $3.01\pm.17$, but analysis of variance showed no systematic dependence on cooking conditions. The CC/B ratio did, however, vary significantly from cell to cell, and was higher at the chip face than at its center.

EFFECTS OF PH AND TIME IN LIQUID PHASE COOKS

Treatment means from analysis of chips from the liquid phase cooks are shown in Table 3 and the corresponding analyses of variance are appended as Tables A4 through A6. The mean number of secondary wall sulfur counts, S, increased with an increase in cooking time and was higher at the two alkaline pH levels than in acid medium. More than half of the sulfur observed after one hour at maximum temperature was present at the end of the heat-up period. Analysis of variance (Table A4) confirmed the significance of the time and pH effects but did not detect any significant interaction, indicating that the effect of extending the time at maximum temperature is independent of pH. This, in turn, suggests that additional sulfur introduced as a result of increasing the pH was introduced rapidly during the heat-up period. The analysis of variance also revealed a high degree of variability between cells, an observation which parallels that noted above in the discussion of the vapor phase cooks. Unlike the vapor-phase cooks, however, the liquid-phase cooks exhibited significant chip-to-chip variability in the amount of sulfur incorporated by the secondary wall. This suggests that individual chips differ in

resistance to transport from the bulk liquid to the chip interior and implies a further limitation on uniformity of treatment in commercial processes.

A major difference between the vapor-phase and liquid-phase cooks was the control over the sulfur distribution afforded by the latter. The A/B ratio was significantly lower when the sulfonating treatment was conducted under alkaline conditions. This is an important observation, both because it suggests a means of manipulating and optimizing the distribution and because it provides evidence for the hypothesis that the secondary wall gradient arises from limitations on diffusion within the secondary wall. The alkali-swollen cell wall may be expected, by virtue of its more open structure, to offer less resistance to diffusion and thereby to give rise to the observed flatter gradient. In addition, yield loss during the 60-minute alkaline cooks may also be expected to have increased diffusivity, which is consistent with the observation of flatter gradients in chips from these cooks. A final point worth noting in this regard is that any lignin condensation and crosslinking that may have occurred under acid conditions would probably reduce diffusivity.

Extending the time at maximum temperature had no significant effect, an observation which is not inconsistent with the limited diffusion hypothesis if it is assumed that reaction was not complete at the longer time and that the rates of diffusion and chemical reaction are of comparable magnitude. Another departure from the pattern displayed by the vapor-phase cooks was the reduced variability in A/B ratio within the same cell wall (between scans). The variability between cells was again low but, because of the lower within-wall variability, was too high to be explainable on the basis of within-cell variability alone. There was also significant variability in A/B ratio between chips. There was, however, no systematic difference between locations near the chip face and at the chip center.

Unlike the A/B ratio, the CC/B ratio was not significantly affected by pH and did display a significant time effect, exhibiting a decrease during the period at maximum temperature. The lack of a pH effect indicates that alkali-enhanced diffusivity of the secondary wall enhances sulfonation of the CC and outer secondary wall regions to the same extent. It follows that diffusion within the middle lamella is not subject to the same limitations as diffusion in the secondary wall. Further evidence for this conclusion is provided by the general lack of observed sulfur gradients within the CC regions, as exemplified by Figure 2(b).

The negative effect of time on CC/B may be due to differences in the capacity of middle lamella and secondary wall lignin for sulfonation.

CC/B was also observed to vary significantly from one cell to another, which paralleled the corresponding observation in chips from the vapor phase cooks, and also from one chip to another.

observed. This variability may be contrasted with the near constancy of the observed A/B ratios from cell to cell.

An example of lignin distribution data obtained at 280 nm by UV microspectrophotometry is shown in Figure 7. Salient features were the middle lamella peak, the generally flat S2 distribution and the S3 peak.

In summary, the results of our efforts to determine lignin distribution in the cell wall suggest that a relatively high concentration in the S3 layer contributes to the observed sulfur gradient, but the absence of a consistent or pronounced S2 lignin gradient indicates that other factors are involved.

LIGNIN REACTIVITY AS A POSSIBLE SOURCE OF THE SECONDARY WALL SULFUR GRADIENT

Much of what is known about lignin reactivity differences across the cell wall concerns differences between the secondary wall and middle lamella. On the other hand, to explain the observed sulfur profiles on the basis of reactivity, it would be necessary to demonstrate the existence of corresponding reactivity gradients within the secondary wall. Although these have been the subject of speculation, there is little evidence for their existence.

Several studies of sprucewood have provided evidence for secondary wall phenolic hydroxyl contents that are twice those in the middle lamella[14,15], favoring sulfonation of the secondary wall. In addition, Berry and Bolker[16] determined the degree of cross linking in middle lamella lignin to be twice that in secondary wall lignin, and Westermark[17] showed that middle lamella lignin is more condensed. It is likely[18] that these differences are due to environmental factors operative during lignification. It is therefore possible that these environmental factors extend their influence into the outer secondary wall. On the other hand, a number of studies[4,12] which have found uniform distributions of bound sulfur or bromine across the cell have thereby supplied indirect evidence for uniform reactivity.

DIFFUSIONAL RESISTANCE AS A POSSIBLE SOURCE OF THE SECONDARY WALL SULFUR GRADIENT

Resistance to diffusion at first appears an unlikely source of the gradient because of the extremely small diffusional path, only a few microns, presented by the fiber wall in its thickness direction. Nevertheless, there are several factors that combine to reduce rates of diffusion in porous media which, when combined, may slow the transport of sulfite ions sufficiently to give rise to the observed gradients. Furthermore, such an effect may be enhanced by the simultaneous occurrence of a relatively fast chemical reaction.

A DYNAMIC MODEL OF CELL WALL DIFFUSION AND REACTION

To better understand the potential for intrafiber diffusion to become a controlling factor, we constructed a dynamic model that could be used to simulate diffusion with simultaneous chemical reaction within the cell wall. An important parameter in this model is the effective diffusivity of sodium sulfite; to estimate it, we conducted an extensive literature review and theoretical analysis.

The model is based on the one-dimensional system shown in Figure 8. The lumen is assumed to be initially filled with liquor, and vapor-phase conditions are assumed so that the only liquor available is that contained by the lumen and the adjacent fiber wall. The model describes the development of profiles for sulfite ion concentration, S, and bound sulfur concentration, S*, across the cell wall by simulating the process of unsteady state diffusion with simultaneous chemical reaction.

The model equations are

$$\delta S/\delta t = D_{eff} (\delta^2 S/\delta x^2) + R \qquad (1)$$

$$R = (\delta S/\delta t)_{rxn} = -(\delta S^*/\delta t) = -k(S) (S_p - S^*) \qquad (2)$$

where R is the reaction term, k is the second order rate constant, S_p is the maximum possible bound sulfite concentration, and D_{eff} is the effective diffusivity of sulfite ion in the cell wall. This last parameter can depend on a variety of factors which include the diffusivity of the sulfite ion in water, the effects of sulfite ion hydration, porosity and tortuosity of the cell wall, viscous drag, adsorption, and electrostatic effects.

In order to solve these equations, a number of initial and boundary conditions were established. Initially, the lumen contains a sodium sulfite solution of known concentration (S_o). The wall is assumed to be thoroughly impregnated with the liquor at the outset, and none of it has reacted. In other words,

$$\text{At } t = 0, \qquad S_L = S_{wall} = S_o$$
$$S^* = 0 \qquad (3)$$

where S_L is the sulfite ion concentration in the lumen at any time, t, during the course of the cook. The upcoming discussion reveals that diffusivity across the lumen is much higher than that across the cell wall. As a consequence, any sulfite ion gradients across the lumen are probably negligible when compared to those across the cell wall, so the sulfite ion distribution across the lumen is assumed to be uniform.

During the cook, the system is subject to the following boundary conditions:

At $x = 0$, $S = S_L$

$$\delta S^*/\delta t = k(S_L)\,(S_p - S^*) \qquad (4)$$

At $x = L$, $\delta S/\delta x = 0$

$$\delta S^*/\delta x = 0 \qquad (5)$$

The boundary condition for S^* at $x = 0$ is simply the solution of the reaction term (equation 2) for $S = S_L$. The boundary conditions for $x = L$ are based on the assumption of symmetry between the profiles of adjacent walls.

The model assumes a uniform lignin concentration across the S2 layer, an S3 lignin concentration that is 1.4 times as high as in the S2, and a middle lamella lignin concentration that is four times as high as in the S2 layer. The middle lamella lignin is assumed to react more slowly than secondary wall lignin by a factor of 1.5.

The partial differential equations are numerically solved by transforming them to ordinary differential equations, as described in detail elsewhere[7].

Bulk Diffusivity and Effective Diffusivity

The diffusion of ions through water-saturated porous solids is slower than through bulk water. Two kinds of factors are responsible for the difference: mechanical blocking and hindrance of diffusion within pores. Both must be taken into account when modeling diffusion in the fiber wall. The approach we have taken is to first use established correlations to estimate the diffusivity of sodium sulfite in water and its dependence on temperature and concentration, and then to apply correction factors for blocking and hindrance based on analysis of the literature.

The bulk diffusivity of sodium sulfite was calculated from equivalent ionic conductivities[19] using the Nernst-Haskell equation[20]. The value obtained was 1.23×10^{-5} cm^2/sec at 25^oC and infinite dilution. Its temperature dependence was modeled by the Stokes-Einstein equation[21], and its concentration dependence was estimated by approximating the activity coefficient of sodium sulfite with that of sodium sulfate.

Mechanical Blocking

Corrections for mechanical blocking, in essence, account for collisions of the diffusing ions with the solid. They reflect the expectation that diffusivity will be directly proportional to porosity, or void fraction, and inversely proportional to the tortuosity of the pores. The former is available from fiber saturation point data, but the latter is more elusive. In principle, its estimation requires a detailed knowledge of fiber wall structure. In practice, it can be estimated by making a series of

reasonable assumptions, provided that a conceptual model of the fiber wall is available to serve as a starting point. The model proposed by Kerr and Goring[22] was used for this purpose. These authors consider the cell wall to consist of longitudinally oriented groups of cellulose protofibrils embedded in a lignin-hemicellulose matrix.

The effective tortuosity of such a structure may be considered to be the product of three component tortuosities, one characterizing the matrix, one associated with the protofibrils, and one reflecting the effect of "dead ends" or obstructed pores. A tortuosity value of three is appropriate for a structure characterized by randomly oriented pores, since the probability of any given pore being oriented primarily in the diffusional direction is one-third. It seems reasonable to assign this value to the presumably amorphous matrix material.

The second component tortuosity, that presented by the protofibrils, was assigned a value of two by Favis and Goring[23], who assumed that crystalline cellulose is impenetrable and that the protofibrils are completely crystalline. We relaxed the latter assumption somewhat to arrive at a value of 1.67.

The final component, that due to impassable pores, was estimated as the fraction of pores too small to accommodate the hydrated sulfite ion. This was calculated from the pore size distribution data of Stone and Scallan[24] as described by Heazel[7]. The resulting value was 6.9. The effective tortuosity was then obtained as the product of the three component values, 34.5.

Hindrance of Diffusion in Pores

Even if all the pores in the fiber wall were free of any tortuosity by being perfectly straight and aligned with the direction of diffusion, and if all were free of blockage and of sufficient diameter to allow the passage of sulfite ions, the rate of diffusion may still be less than predicted on the basis of bulk diffusivity and void fraction. The reason is that there exists another set of phenomena which have the effect of slowing diffusion within pores. These are the existence of an impenetrable monolayer of water on the pore wall[25], steric effects that reduce the concentration of solute in the pore[25], hydrodynamic effects[26,27], electrostatic effects[28,29], enhanced viscosity of water within pores[30], and solute adsorption[31].

Estimation of Effective Diffusivity

Corrections for electrostatic, steric and hydrodynamic effects, as well as a correction for the existence of a water monolayer have been estimated by Heazel[7] on the basis of an analysis of the literature referred to above. No attempt was made to account for the effects of solute adsorption and enhanced viscosity. These corrections were combined with the above tortuosity estimates to arrive at an effective diffusivity of 2×10^{-10} cm^2/sec for sodium sulfite in 1.03M solution at 140^oC.

Model Results

The model was used to simulate chip sulfonation under various conditions of temperature and initial concentration of sodium sulfite. Some of the results obtained are presented in Figures 9-11.

In the early stages of the cook, lignin consumes sulfite initially in the cell wall, establishing a concentration difference between the lumen and the cell wall, which initiates diffusion of sulfite ions into the wall. The combination of rapid reaction and relatively slow diffusion results in the development of a gradient in the concentration of sulfite ions, as shown in Figure 9. Since this concentration is the driving force for lignin sulfonation, a corresponding gradient in bound sulfur develops, as shown in Figure 10. Both gradients become steeper as the supplied value of effective diffusivity is decreased; the value estimated as outlined above would correspond to a noticeable gradient and a calculated A/B ratio of 1.7. This is similar to the experimentally observed values, although it is strongly dependent on the assumed relationship between S3 and S2 lignin concentrations. More significantly, the model predicts a decline in A/B ratio at a fixed cooking time as the sulfite concentration is increased. This behavior was experimentally observed as shown by the results of our regression analysis and illustrated in Figure 11, which compares the model predictions with the data from some of our vapor-phase cooks[5]. The ratio declines with increasing concentration because the corresponding higher bound sulfite levels reduce the number of available sites toward the end of the cook. This reduces the reaction rate, allowing more sulfite ions to diffuse into the outer secondary wall where they react with available sites on the lignin there.

In summary, the modeling part of this study shows that resistance to diffusion within the cell wall may contribute to the development of bound sulfur gradients within the secondary wall. The mathematical model simulated the experimental data reasonably well, and current knowledge of diffusion in porous media suggests that the effective diffusivities used in the model are realistic.

CONCLUSIONS

The work presented in this paper represents a significant contribution to our understanding of cell wall sulfur distribution in sulfonated wood. This work has provided unique findings concerning the nature of these distributions and how they can be manipulated. A fundamental knowledge of the origins of the observed distributions was also acquired.

The observed bound sulfur distributions across the cell wall were characterized by a nonuniform secondary wall distribution and considerably higher levels in the middle lamella. The secondary wall distribution consisted of relatively high sulfur levels toward the lumen and a decline in sulfur levels across the cell wall to a

chips. The sulfur content was determined by Schoniger flask combustion-ion chromatography[33].

The treated chips were dehydrated and impregnated with Spurr resin. Transverse 250 nm sections were prepared and mounted on 200-mesh ultra-high-transmission nickel grids. Scanning transmission electron microscopy with energy dispersive spectrometry (STEM-EDS) was used to obtain linescans that consisted of measurements at 64 points, or pixels, across the tangential double-cell wall, from lumen to lumen. Linescans of 10 pixels were also performed across the cell corners. The measurement taken at each point along the linescan was the number of sulfur X-ray counts detected from the K2 sulfur peak (a range of 2.18-2.44 keV in the X-ray spectrum), minus the background. The STEM used was a Jeol JEM 100-CX with an ASID4D scanning unit; it was equipped with a liquid-nitrogen-cooled anticontamination trap to minimize specimen damage and mass loss. The EDS system was a Tracor Northern TN-2000.

Mass loss at shorter time intervals was measured with STEM-EDS timescans, which measured changes in counts from a spot or area as a function of time. Time increments ranging from $1X10^{-4}$ seconds to over 6 seconds were available, but the longer time increments were generally necessary in order to obtain a sufficient number of counts. Measurements were generally made by blindly approaching the area to be tested and starting the timescan the moment this area was first exposed to the beam. Unlike the linescan data, timescans could only collect data for one element at a time.

The loss of sulfur was measured by monitoring changes in the Ka sulfur peak (2.18 to 2.44 keV). Since the timescans can only collect one set of data at a time, background counts could not be simultaneously collected and subtracted from the total sulfur data to obtain net sulfur data. To obtain net sulfur mass loss data, total mass and total sulfur timescans were collected from two adjacent areas, and a spectrum was then collected from one of these areas to give total sulfur (TS), background (BG), and net sulfur (NS) data for an area which had undergone mass loss. Since the background region (1.92 to 2.18 keV) is part of the continuum, the percent loss of background should be comparable to percent mass loss. The net sulfur loss can be obtained from these data using the following relation,

$$[\text{counts}/(100-ML)]TS = [\text{counts}/(100-ML)]BG = [\text{counts}/(100-ML)]NS$$

where ML is the percent mass loss of the element in question. The counts in each term are the counts from the spectrum.

For determinations of lignin distribution, thin sections were prepared and mounted on grids prior to examination by ultraviolet (UV) microscopy. UV microscopy was performed on two separate pieces of equipment: the UV microscope at the U.S. Forest Products Lab in Madison and a Zeiss UMSP-80 UV microscope at Zeiss, Inc. The work at the Forest Products Lab involved taking photos of samples irradiated

under a 300 nm UV light source and then collecting densitometer tracings across the cell wall images on the negatives. The UV microscope at the Forest Products Lab was an old Zeiss microscope equipped with a monochromator and a 35 mm camera. Mounted sections from chip 2 of sample 1 and sample 3-EM were placed between a quartz slide and cover slip in an immersion-glycerin solution and examined under a 100X objective at a 300 nm wavelength. While UV absorbance work on lignin is generally done at 280 nm, the choice of a 300 nm wavelength for this work was based on a previous finding that Spurr resin absorbs significantly below 290 nm. Subsequent work in this study confirmed this finding, but also found some absorbance above 290 nm. Three areas of approximately 75 X 75 μm were photographed from each sample on Kodak technical pan 2415 film. The exact magnification of the photos is not known, but it was probably around 500X.

After the film was developed, two negatives, representing two areas in the chip, were chosen for each sample. Densitometer traces were obtained from two walls in each of the negatives. This work was performed on a Joyce Loebl double-beam microdensitometer, which scanned a narrow beam of light across the cell walls on the negatives and recorded density variations, representing variations in lignin concentration, on a piece of graph paper. The settings used on the microdensitometer could theoretically yield spatial resolutions in the cell wall of 0.15 μm.

The Zeiss UMSP-80 is a state-of-the-art UV microscope which offers several advantages over the other equipment available. These include the ability to collect linescan and spectral data, and a low signal-to-noise ratio. Data included scans across cell walls at 280 nm and spectral data from the lumen, secondary wall, and cell corner. A special effort was made to obtain good data from the S3 layer. The data from the nonembedded samples consisted of spectra from the cell wall. All data were processed and smoothed by the Lambda-scan program, which was developed by Zeiss for this purpose.

APPENDIX

Table A1: AOV table for VP2 cooks; net secondary wall sulfur counts (average net sulfur counts per pixel).

Source	Error Term	Sum of Squares	DF	Mean Square	F	Tail Prob.
Time-temp.	Chip	101841	1	101841	9.68	0.036
Na_2SO_3 conc.	Chip	892316	1	892316	84.85	0.001
Time X Na_2SO_3	Chip	7332	1	7332	0.70	0.451
Chip	Wall	42063	4	10516	0.56	0.832
Location	Wall	41057	1	41057	2.20	0.500
Wall	Scan	428965	23	18651	274.28	0.000
Scan		2183	32	68		

Table A2: AOV table for VP2 cooks; net A/B ratio.

Source	Error Term	Sum of Squares	DF	Mean Square	F	Tail Prob.
Time-temp.	Chip	0.000594	1	.000594	0.01	0.925
Na_2SO_3 conc.	Chip	0.025881	1	.025881	0.43	0.547
Time X Na_2SO_3	Chip	0.000193	1	.000193	0.00	0.958
Chip	Wall	0.239517	4	.059879	0.99	0.445
Location	Wall	0.167383	1	.167383	2.77	0.116
Wall	Scan	1.387641	23	.060332	1.34	0.229
Scan		1.446042	32	.045189		

Table A3: AOV table for VP2 cooks; net CC/B ratio.

Source	Error Term	Sum of Squares	DF	Mean Square	F	Tail Prob.
Time-temp.	Chip	1.927238	1	1.92724	2.77	0.171
Na_2SO_3 conc.	Chip	1.604022	1	1.60402	2.31	0.204
Time X Na_2SO_3	Chip	1.075369	1	1.07537	1.55	0.282
Chip	Wall	2.783253	4	0.69581	2.02	0.134
Location	Wall	1.768235	1	1.76824	5.11	0.030
Wall	Scan	7.925922	23	0.34461	6.25	0.000
Scan		1.764033	32	0.05513		

Table A4: AOV table for LP1 cooks; net secondary wall sulfur counts (average net sulfur counts per pixel).

Source	Error Term	Sum of Squares	DF	Mean Square	F	Tail Prob.
Time	Chip	3773887	1	3773887	30.30	0.000
pH	Chip	3240628	2	1620314	13.01	0.007
Time X pH	Chip	330565	2	165282	1.33	0.333
Chip	Wall	747216	6	124536	4.31	0.039
Location	Wall	6	1	6	0.00	0.999
Wall	Scan	1011578	35	28902	69.31	0.000
Scan		20012	48	417		

Table A5: AOV table for LP1 cooks; net A/B ratio.

Source	Error Term	Sum of Squares	DF	Mean Square	F	Tail Prob.
Time	Chip	0.097219	1	.09722	0.67	0.445
pH	Chip	2.334710	2	1.16736	8.03	0.020
Time X pH	Chip	0.510797	2	0.25540	1.76	0.251
Chip	Wall	0.872090	6	0.14535	3.21	0.014
Location	Wall	0.090221	1	0.09022	2.00	0.187
Wall	Scan	1.582616	35	0.04522	4.61	0.000
Scan		0.470653	48	0.00981		

Table A6: AOV table for LP1 cooks; net CC/B ratio.

Source	Error Term	Sum of Squares	DF	Mean Square	F	Tail Prob.
Time	Chip	7.773678	1	7.77368	6.94	0.039
pH	Chip	7.107676	2	3.55384	3.17	0.115
Time X pH	Chip	1.105924	2	0.55296	0.49	0.633
Chip	Wall	6.721078	6	1.12018	3.85	0.005
Location	Wall	0.143840	1	0.14384	0.49	0.492
Wall	Scan	10.182418	35	0.29093	24.75	0.000
Scan		0.564185	48	0.11754		

LITERATURE CITED

1. T. Iwamida, Y. Sumi, and J. Nakano, *Cellulose Chem. and Tech.* 14:253(1980).

2. D. Atack, C. Heitner, and A. Karnis, *Svensk Papperstidning,* "Ultra-high yield pulping of eastern black spruce, Part 2." 83(5):133(1980).

3. J.J. Kolar, B.O. Lindgren, and E. Treiber, *Svensk Papperstid.* 85(3):R21(1982).

4. R.P. Beatson, C. Gancet, and C. Heitner, *Tappi J.,* "The topochemistry of black spruce sulfonation." 67(3):82(1984).

5. T.E. Heazel and T.J. McDonough, *Tappi J.,* 71(3):129(March 1988).

6. M. Mary, J.-F. Revol, and D.A.I. Goring, *J. Appl. Polymer Sci.,* "Mass loss of wood and its components during transmission electron microscopy." 31:957 (1986).

7. T.E. Heazel, Cell wall sulfur distribution in sulfonated southern pine latewood, Ph.D. thesis, The Institute of Paper Chemistry (July, 1988).

8. R.P. Beatson, C. Heitner, and D. Atack, *Journal of Wood Chemistry and Technology,* "Sulphonation of eastern black spruce chips," Part 2. 4(4):w39(1984).

9. P. Engstrand, L.-A. Hammar, and M. Htun, "The kinetics of sulfonation reactions on Norwegian spruce," Proceedings of the International Symposium on Wood and Pulping Chemistry, Vancouver, Canada, 1985. p. 275.

10. R.A. Parham and W.A. Cote, *Wood Science and Technology,* "Distribution of Lignin in normal and compression wood of Pinus taeda L." 5:49(1971).

11. I.B. Sachs, I.T. Clark, and J.C. Pew, *J. Polymer Science,* "Investigation of lignin distribution in the cell wall of certain woods," Part C. 2203(1963).

12. S. Saka, R.J. Thomas, and J.S. Gratzl, "Lignin distribution in Douglas fir and loblolly pine as determined by energy dispersive x-ray analysis," in Proceedings of the International Symposium on Wood and Pulping Chemistry, Stockholm, June 9-12, 1981. p. 35.

13. S. Saka and R.J. Thomas, *Wood Science and Technology,* "A study of lignification in loblolly pine tracheids by the SEM-EDXA technique." 16:167(1982).

14. H.-L. Hardell, G.J. Leary, M. Stoll, and U. Westermark, *Svensk Papperstid.,* "Variations in lignin structure in defined morphological parts of spruce." 83(2):44(1980).

15. P. Whiting, and D.A.I. Goring, *Paperi ja Puu*, "Phenolic hydroxyl analysis of lignin by pyrolytic gas chromatography." 64(10):592(1982).

16. R. Berry and H.I. Bolker, "The topochemical effect in acid sulphite delignification: a theoretical analysis," Canadian Wood Chemistry Symposium, Niagara Falls, September 13-15, 1982, p. 137.

17. U. Westermark, *Wood Science and Technology*, "The occurrence of p-hydroxyphenyl-propane units in the middle lamella lignin of spruce (Picea abies)." 19:223(1985).

18. N. Terashima, *Journal of the Japanese Wood Research Society*, "Cell wall formation in tree xylem." 33(8):615(1987).

19. CRC Handbook of Chemistry and Physics, 65th edition. Boca Raton, FL, Chemical Rubber Company Press, 1984.

20. R.C. Reid, J.M. Prausnitz, and T.K. Sherwood, The Properties of Gases and Liquids, 3rd edition. New York, McGraw-Hill, 1977.

21. E.L. Cussler, Diffusion: Mass Transfer in Fluid Systems, Cambridge, Cambridge University Press, 1984.

22. A.J. Kerr, and D.A.I. Goring, *Cellulose Chemistry and Technology*, "Ultrastructural arrangement of the wood cell wall." 9(6):563 (1975).

23. B.D. Favis and D.A.I. Goring, *Journal of Pulp and Paper Science*, "A model for the leaching of lignin macromoleculse from pulp fibres." 10(5):J139 (1984).

24. J.E. Stone and A.M. Scallan, *Cellulose Chemistry and Technology*, "A structural model for the cell wall of water swollen wood pulp fibers based on their accessibility to macromolecules." 2(3):343 (1968).

25. M. Ternan, *The Canadian Journal of Chemical Engineering*, "The diffusion of liquids in pores." 65(2):244 (1987).

26. W.M. Deen, *AIChE Journal*, "Hindered transport of large molecules in liquid-filled pores." 33(9):1409 (1987).

27. H. Wang and R. Shalak, *Journal of Fluid Mechanics*, "Viscous flow in a cylindrical tube containing a line of spherical particles." 38(1):75 (1969).

28. S. Takigami and Y. Nakamura, *Journal of Applied Polymer Science*, "Permeability of solutes through cellophanes grafted with vinyl monomers, II. Diffusion of potassium chloride through cellophanes grafted with acrylic acid." 24(6):1429 (1979).

29. T. Ueda, N. Kamo, N. Ishida, and Y. Kobatake, *The Journal of Physical Chemistry*, "Effective fixed charge density governing membrane phenomena. IV. Further study of activity coefficients and mobilities of small ions in charged membranes." 76(17):2447 (1972).

30. J.N. Israelachvili, *Journal of Colloid and Interface Science*, "Measurement of viscosity in very thin films." 110(1):263 (1986).

31. C.N. Satterfield, C.K. Colton, and W.H. Pitcher, *AIChE Journal*, Restricted diffusion in liquids within fine pores. 19(3):628 (1973).

32. G.V. Palmrose, *Paper Trade J.* 100(3):38(1935).

33. R.S. Colaruotola, *Analytical Chemistry*. 49(6):884 (1977).

ACKNOWLEDGMENTS

We thank John D. Litvay and William J. Whitsitt for valuable discussions, and Terry Conners, Mary Block, Ellen Foxgrover and Hilkka Kaustinen for their skilled technical assistance. We also thank the member companies of The Institute of Paper Chemistry, now The Institute of Paper Science and Technology, for their support of this work.

Portions of this work were used by T.E.H. as partial fulfillment of the requirements for the Ph.D. degree at the Institute of Paper Science and Technology.

Table 1: Final pH, yield, and sulfur content results from high-yield sulfite cooks.

Experiment	Time, min.	Temp., °C	Na_2SO_3 conc., mole/l	Initial pH	Final pH	Yield %ODT wood	Sulfur Content %ODT wood
VP2	5	160	0.48	11.5	6.12	99.3	0.30
VP2	5	160	1.03	11.5	7.01	99.0	0.46
VP2	20	140	0.48	11.5	6.75	99.6	0.32
VP2	20	140	1.03	11.5	6.98	99.5	0.48
LP1	0	140	1.03	3.3	4.26	98.8	0.44
LP1	0	140	1.03	10.0	8.39	97.3	0.61
LP1	0	140	1.03	12.5	10.52	99.8	0.58
LP1	60	140	1.03	3.3	4.87	98.3	0.64
LP1	60	140	1.03	10.0	8.46	94.8	0.81
LP1	60	140	1.03	12.5	10.00	90.1	0.78

Table 2: VP2 treatment means for various parameters used to describe the degree of sulfonation or relative degree of sulfonation of different cell wall layers. Sulfur content data from Table 1 included. 95% C.I. = 95% confidence interval.

Time, min.	Temp., °C	Na_2SO_3 conc., mole/l* Liquor	Effective	Parameter A	B	CC	A/B	CC/B	S	Sulfur Content
5	160	0.48	0.26	418	252	808	1.66	3.21	278	0.30
5	160	1.03	0.55	698	448	1396	1.63	3.15	492	0.46
20	140	0.48	0.26	253	156	477	1.66	3.12	176	0.32
20	140	1.03	0.55	621	388	975	1.62	2.54	434	0.48
		MEAN ± 95% C.I.					1.64 ±.06	3.01 ±.17		

* The effective Na_2SO_3 conc. accounts for liquor dilution by chip moisture within the chip.

Table 3: LP1 treatment means for various parameters used to describe the degree of sulfonation of relative degree of sulfonation of different cell wall layers. Sulfur content data from Table 1 included.

Time, min.	Liquor pH	Parameter A	B	CC	A/B	CC/B	S	Sulfur Content
0	4.3	608	345	1064	1.76	3.07	394	0.44
0	8.4	864	625	1796	1.36	2.88	672	0.61
0	10.5	1062	707	1826	1.50	2.57	781	0.58
60	4.3	1067	637	1724	1.69	2.77	714	0.64
60	8.4	1696	1140	2316	1.48	2.05	1234	0.81
60	10.5	1277	1021	2001	1.26	1.99	1087	0.78
	MEAN				1.51	2.55		

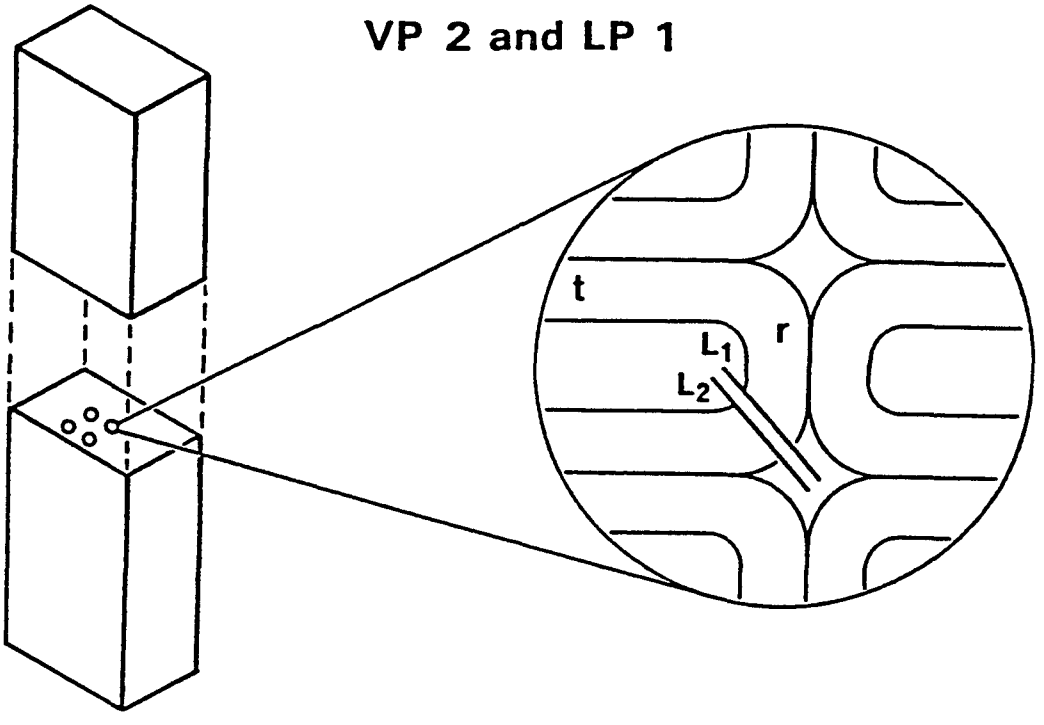

Figure 1: Locations of scans within the chip and walls of the VP2 and LP1 cooks.

a).

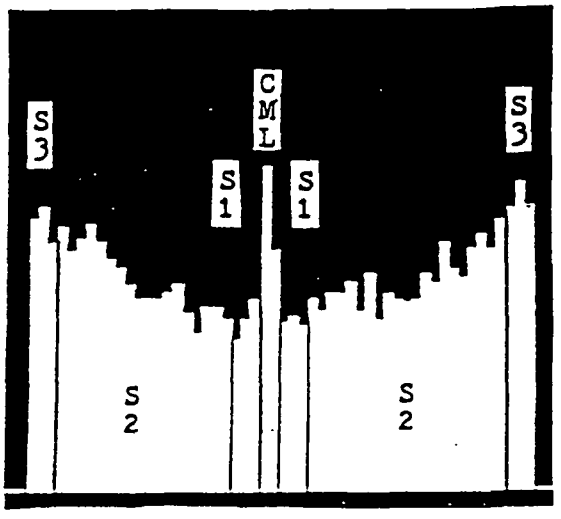

b).

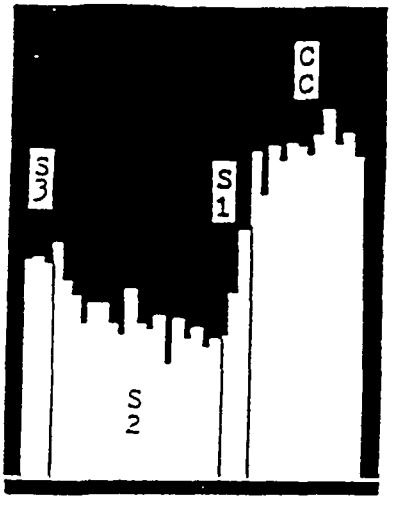

Figure 2: Typical linescan histograms displaying the secondary wall gradient and higher sulfur levels in the middle lamella; (a) double-wall scan; (b) cell corner scan.

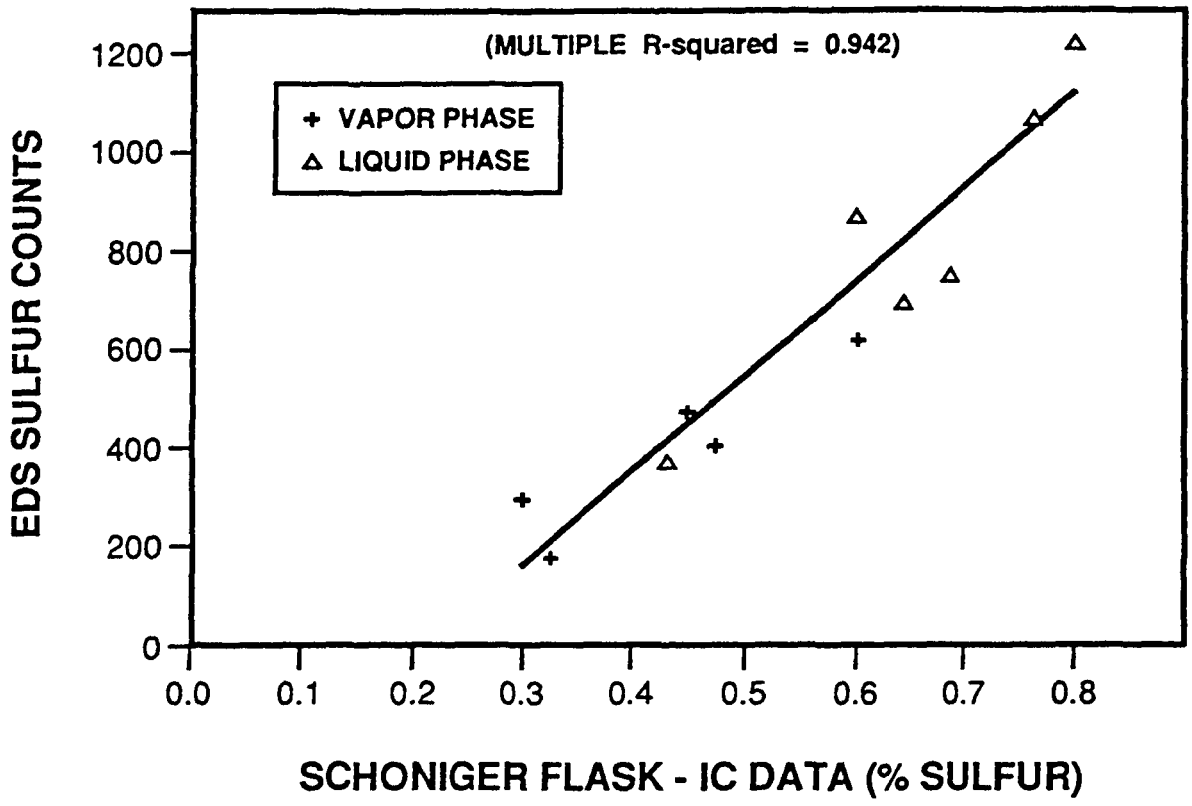

Figure 3: Plot comparing mean secondary wall net sulfur count data with Schoniger flask/ion chromatography sulfur contents.

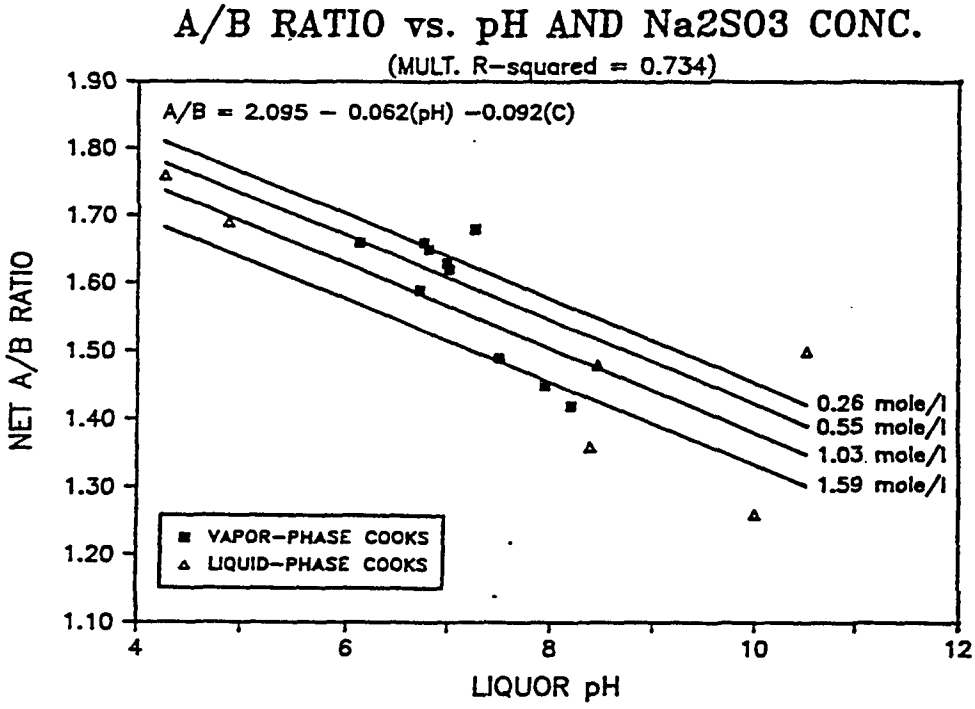

Figure 4: Multiple linear regression of A/B ratio vs. liquor pH (abscissa) and liquor sodium sulfite (Na_2SO_3) concentration (parallel lines).

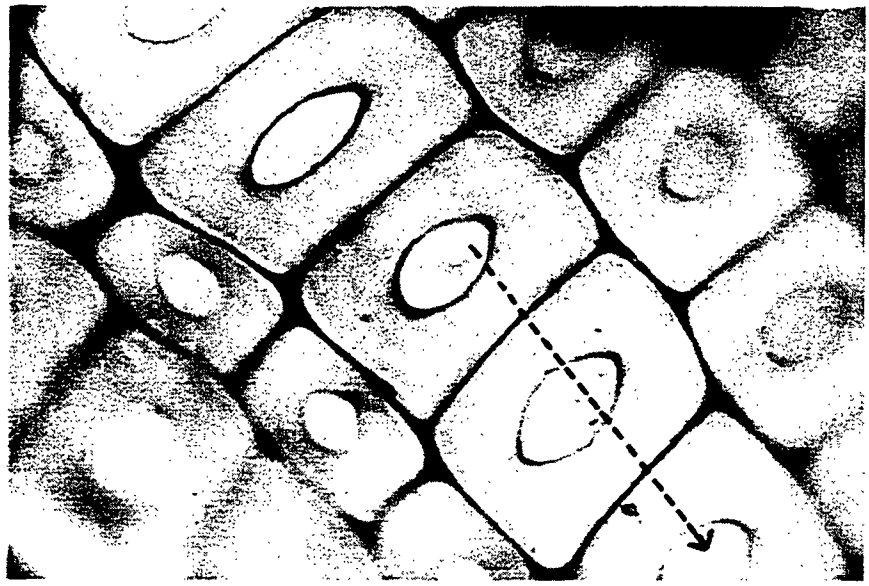

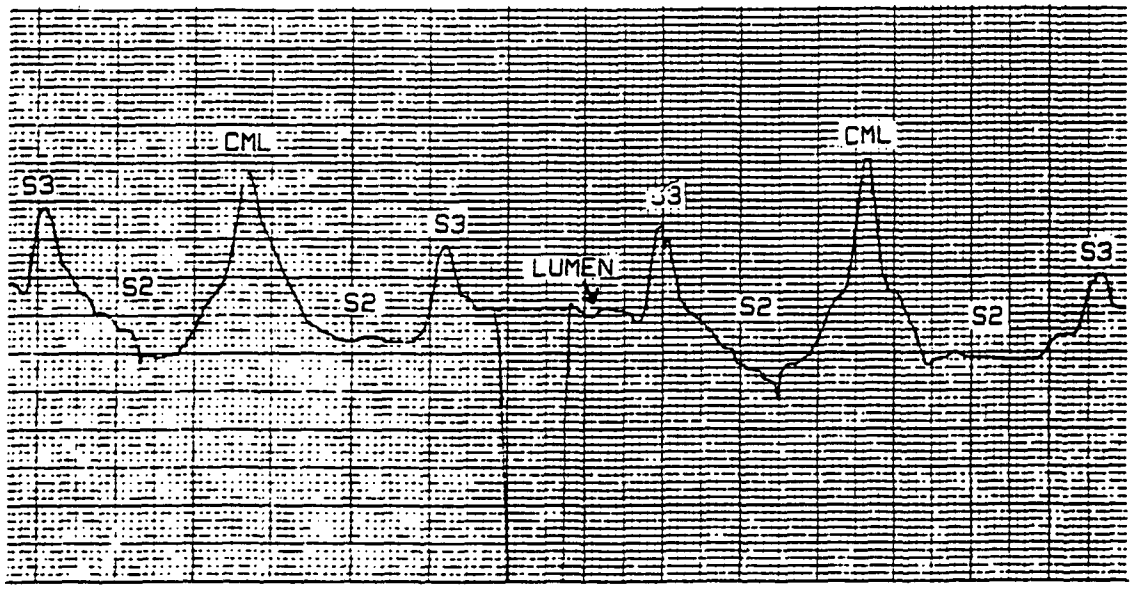

Figure 5a, 5b: Densitometer trace from the above cell wall.

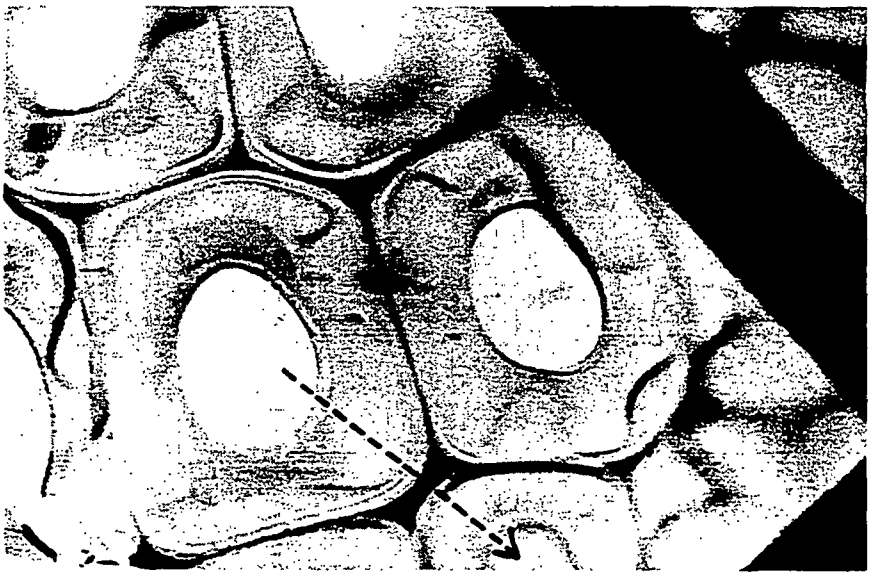

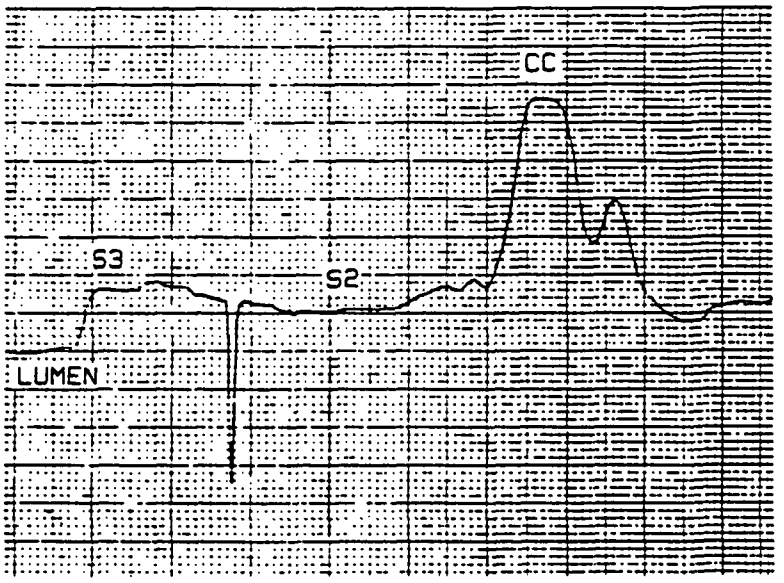

Figure 6a, 6b: Sample 1.

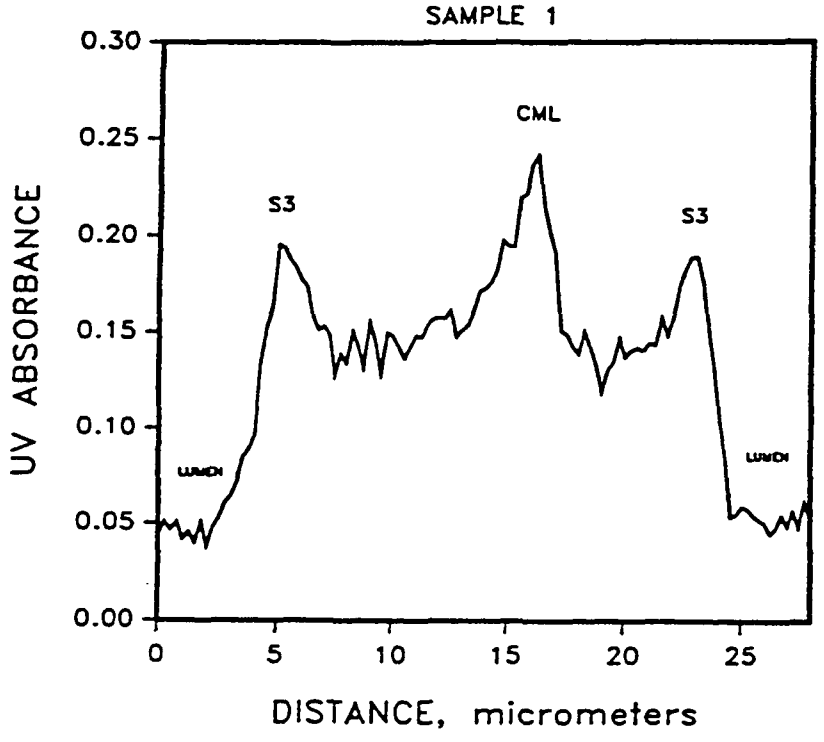

Figure 7: Lignin distribution obtained by UV microspectrophotometry. Sample 1, chip 1.

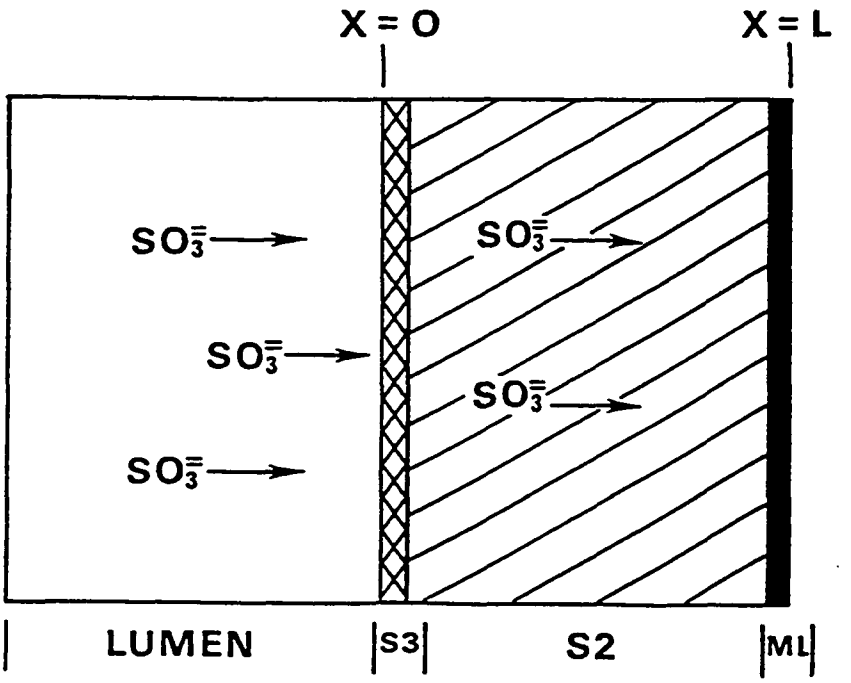

Figure 8: System used for diffusion modelling. Sodium ions, which are diffusing with the sulfite ions, are not shown.

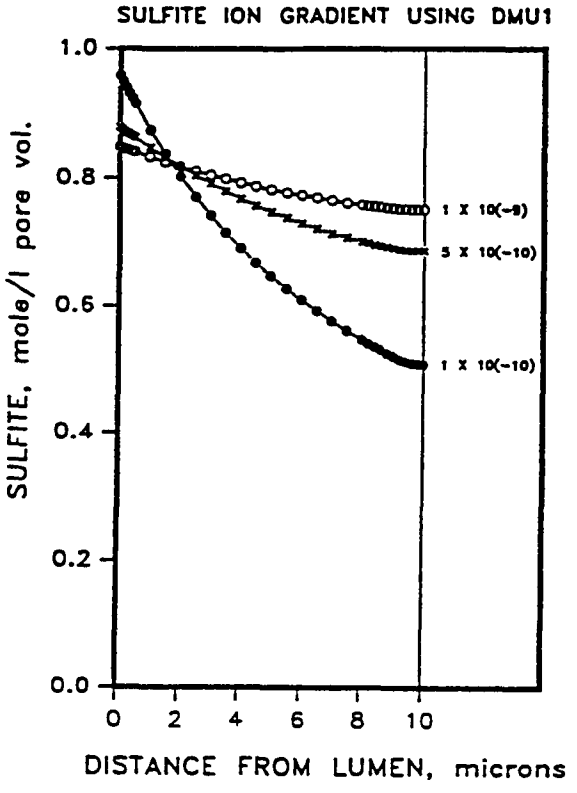

Figure 9: Sulfite ion distribution at different D_{eff} values. Data generated from program DMU1 for a 20-minute, 134°C vapor-phase cook using 1.03 molar sodium sulfite. D_{eff} in cm^2/sec.

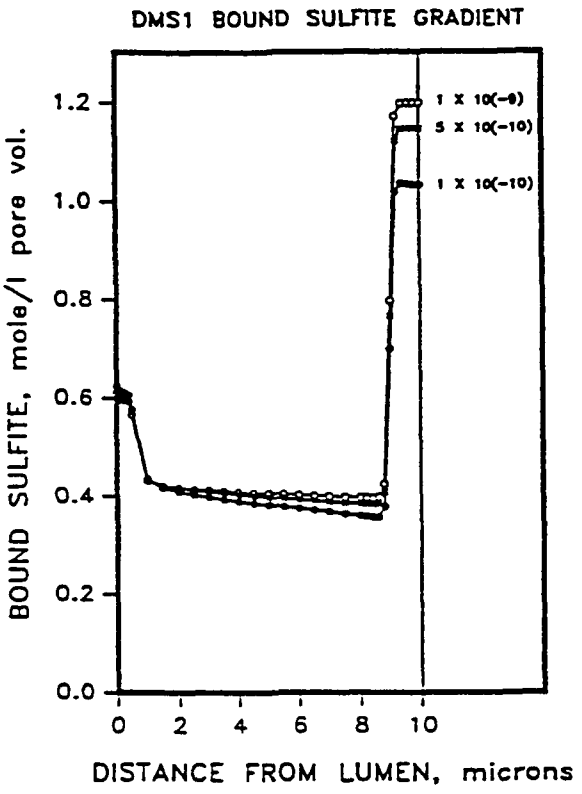

Figure 10: Bound sulfur distribution at different D_{eff} values. Data generated from program DMS1 for a 20-minute, 134°C vapor-phase cook using 1.03 molar sodium sulfite. D_{eff} in cm^2/sec.

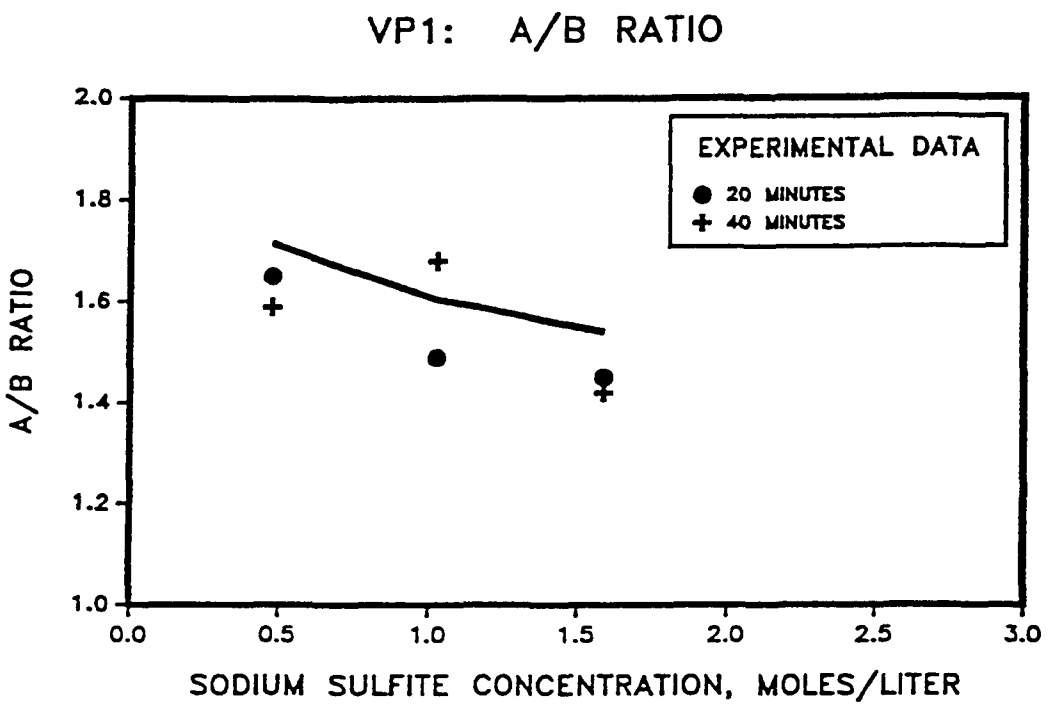

Figure 11: Comparison of experimental and generated A/B ratios for the VP1 cooks. Points represent experimental data. Solid line represents generated data.